Simultaneous Ferromagnetic Metal-Semiconductor Transition in Electron-Doped EuO

Michael Arnold and Johann Kroha

Physikalisches Institut, Universität Bonn, Nussallee 12, 53115 Bonn, Germany

(Received 3 August 2007; published 30 January 2008)

We present a general framework to describe the simultaneous para-to-ferromagnetic and semiconductor-to-metal transition in electron-doped EuO. The theory correctly describes detailed experimental features of the conductivity and of the magnetization, in particular, the doping dependence of the Curie temperature. The existence of correlation-induced local moments on the impurity sites is essential for this description.

DOI: 10.1103/PhysRevLett.100.046404 PACS numbers: 71.30.+h, 72.20.−i, 75.20.Hr

At room temperature stoichiometric europiumoxide (EuO) is a paramagnetic semiconductor which undergoes a ferromagnetic (FM) transition at the Curie temperature of $T_C = 69$ K. Upon electron doping, either by O defects or by Gd impurities, this phase transition turns into a simultaneous ferromagnetic and semiconductor-metal (SM) transition with nearly 100% of the itinerant charge carriers polarized and a sharp resistivity drop of 8 to 13 orders of magnitude, depending on sample quality [1–4]. Concomitant with this transition is a huge colossal magnetoresistance effect [5], much larger than in the intensely studied manganates [6]. These extreme properties make electron-doped EuO interesting for spintronics applications. Known since the 1970s, these features have therefore recently stimulated more systematic experimental studies with modern techniques and improved sample quality [4,7,8] as well as theoretical calculations [9,10].

In pure EuO the FM ordering is driven by the Heisenberg exchange coupling between the localized Eu $4f$ moments with spin $S_f = 7/2$ [11]. Upon electron doping, above T_C, the extra electrons are bound in defect levels situated in the semiconducting gap, and the transition to a FM metal occurs when the majority states of the spin-split conduction band shift downward to overlap with the defect levels. Although this scenario is widely accepted, several questions of fundamental as well as applicational relevance have remained poorly understood. (1) Why does the magnetic ordering of the Eu $4f$ system occur simultaneously [4] with the SM transition of the conduction electron system? (2) What is the order of the transition? While the magnetic ordering of the $4f$ system should clearly be of 2nd order, the metallic transition requires a *finite* shift of the conduction band and, hence, seems to favor a 1st order transition. (3) How can the critical temperature T_C be enhanced by doping for spintronics applications? While in the Eu-rich compound EuO_{1-x} a systematic T_C increase due to the O defects (i.e., missing O atoms) is not observed experimentally [1,2], a minute Gd doping concentration significantly enhances T_C [7,12]. An O defect in EuO_{1-x} essentially binds the two excess electrons from the extra Eu 6s orbital and, therefore, should not carry a magnetic moment. As shown theoretically in Ref. [10], the presence of O defects with twofold electron occupancy does not enhance T_C, in agreement with experiments [1,2]. In the present Letter we focus on the Gd-doped system $Eu_{1-y}Gd_y$ and calculate the temperature and doping dependent magnetization and resistivity from a microscopic model. We find that the key feature for obtaining a T_C enhancement is that the impurities not only donate electrons but also carry a local magnetic moment in the paramagnetic phase.

The model.—A Gd atom substituted for Eu does not alter the $S_f = 7/2$ local moment in the Eu Heisenberg lattice but donates one dopant electron, which in the insulating high-temperature phase is bound in the Gd $5d$ level located in the gap. Therefore, the Gd impurities are Anderson impurities with a local level E_d below the chemical potential μ and a *strong* on-site Coulomb repulsion $U > \mu - E_d$ which restricts their electron occupation essentially to one. The hybridization V with the conduction band is taken to be site diagonal because of the localized Gd $5d$ orbitals. The Hamiltonian for the $Eu_{1-y}Gd_yO$ system then reads

$$H = \sum_{\mathbf{k}\sigma} \varepsilon_{\mathbf{k}} c^\dagger_{\mathbf{k}\sigma} c_{\mathbf{k}\sigma} + H_{\mathrm{cd}} + H_{\mathrm{cf}}, \tag{1}$$

$$H_{\mathrm{cd}} = E_d \sum_{i=1\ldots N_I,\sigma} d^\dagger_{i\sigma} d_{i\sigma} + V \sum_{i=1\ldots N_I,\sigma} (c^\dagger_{i\sigma} d_{i\sigma} + \mathrm{H.c.}) + U \sum_{i=1\ldots N_I} d^\dagger_{i\uparrow} d_{i\uparrow} d^\dagger_{i\downarrow} d_{i\downarrow}, \tag{2}$$

$$H_{\mathrm{cf}} = -\sum_{i,j} J_{ij} \vec{S}_i \cdot \vec{S}_j - J_{\mathrm{cf}} \sum_i \vec{\sigma}_i \cdot \vec{S}_i, \tag{3}$$

where the first term in Eq. (1) denotes conduction electrons with spin σ. The Eu $4f$ moments $\vec{S}_i$ on the lattice sites $i = 1, \ldots, N$ are described in terms of a Heisenberg model H_{cf} with FM nearest and next-nearest neighbor couplings J_{ij} and an exchange coupling J_{cf} to the conduction electron spin operators at site i, $\vec{\sigma}_i = (1/2)\sum_{\sigma\sigma'} c^\dagger_{i\sigma} \vec{\tau}_{\sigma\sigma'} c_{i\sigma'}$, with $c_{i\sigma} = \sum_{\mathbf{k}} \exp(i\mathbf{k}\mathbf{x}_\mathbf{i}) c_{\mathbf{k}\sigma}$ and $\vec{\tau}_{\sigma\sigma'}$ the vector of Pauli matrices. The Gd impurities at the random positions

$i = 1, \ldots, N_I$ are described by $H_{\rm cd}$. For the numerical evaluations we take $U \to \infty$ for simplicity.

For the present purpose of understanding the general form of the magnetization $m(T)$ and the systematic doping dependence of T_C, it is sufficient to treat the $4f$ Heisenberg lattice, $H_{\rm cf}$, on a mean field level, although recent studies have shown that Coulomb correlations in the conduction band can soften the spin wave spectrum in similar systems [13,14]. The effect of the latter on $m(T)$ can be absorbed in the effective mean field coupling of the $4f$ system, $J_{4f} \equiv \sum_j J_{ij}$. We therefore choose J_{4f} such that for pure EuO it yields the experimental value of $T_C = 69$ K [1,2,4,5]. For simplicity, we do not consider a direct coupling $J_{\rm df}$ between the $4f$ and the impurity spins, since this would essentially renormalize $J_{\rm cf}$ only. The indirect RKKY coupling will also be neglected, since for the small conduction band fillings relevant here it is FM, like J_{ij}, but much smaller than J_{ij}.

In the evaluations we use a semielliptical bare conduction band density of states (DOS) with a half width $D_0 = 8$ eV, (consistent with experiment [4]), centered around $\Delta_0 \approx 1.05 D_0$ above the (bare) defect level E_d. The other parameters are taken as $J_{4f} \equiv \sum_j J_{ij} = 7 \times 10^{-5} D_0$, $J_{\rm cf} = 0.05 D_0$, $E_d = -0.4 D_0$, and $\Gamma = \pi V^2 = 0.05 D_0^2$, where $J_{\rm cf} \gg J_{4f}$ because J_{4f} involves a nonlocal matrix element.

Self-consistent theory.—The averaging over the random defect positions is done within the single-site T-matrix approximation, sufficient for dilute impurities. This yields for the retarded conduction electron Green function $G_{c\sigma}(\mathbf{k}, \omega)$ in terms of its self-energy $\Sigma_{c\sigma}(\omega)$,

$$G_{c\sigma}(\mathbf{k}, \omega) = [\omega + \mu - \varepsilon_{\mathbf{k}} - \Sigma_{c\sigma}(\omega)]^{-1}, \tag{4}$$

$$\Sigma_{c\sigma}(\omega) = n_I |V|^2 G_{d\sigma}(\omega) - J_{\rm cf} \langle S \rangle \sigma, \tag{5}$$

where $G_{d\sigma}(\omega)$ is the defect electron propagator and $\langle S \rangle$ is the average $4f$ moment per site. In mean field theory it is obtained, together with the conduction electron magnetization m, as

$$\langle S \rangle = \frac{\sum_S S e^{-\beta(2J_{4f}\langle S \rangle + J_{\rm cf} m) S}}{\sum_S e^{-\beta(2J_{4f}\langle S \rangle + J_{\rm cf} m) S}}, \tag{6}$$

$$m = \frac{1}{2} \int d\omega f(\omega) [A_{c\uparrow}(\omega) - A_{c\downarrow}(\omega)], \tag{7}$$

where $f(\omega)$ is the Fermi distribution function and $A_{c\sigma}(\omega) = -\sum_{\mathbf{k}} {\rm Im} G_{c\sigma}(k, \omega)/\pi$ is the conduction electron DOS of the interacting system.

In order to treat the strongly correlated spin and charge dynamics of the Anderson impurities without double occupancy beyond the static approximation, we use a slave particle representation and employ the noncrossing approximation (NCA) [15]. For EuO the DOS at the Fermi level is so low or even vanishing that the Kondo temperature is well below T_C, and Kondo physics plays no role. In this high-energy regime the NCA has been shown to give quantitatively reliable results [16]. This remains true even for a finite magnetization, where the NCA would develop spurious potential scattering singularities near T_K only [17]. One obtains the following set of equations for $G_{d\sigma}(\omega)$ in terms of the auxiliary fermion and boson propagators $G_{f\sigma}, G_b$, their spectral functions $A_{f\sigma}, A_b$ and their self-energies $\Sigma_{f\sigma}, \Sigma_b$,

$$\Sigma_{f\sigma}(\omega) = \Gamma \int d\varepsilon [1 - f(\varepsilon)] A_{c\sigma}(\varepsilon) G_b(\omega - \varepsilon), \tag{8}$$

$$\Sigma_b(\omega) = \Gamma \sum_\sigma \int d\varepsilon f(\varepsilon) A_{c\sigma}(\varepsilon) G_{f\sigma}(\omega + \varepsilon), \tag{9}$$

$$G_{d\sigma}(\omega) = \int \frac{d\varepsilon}{e^{\beta\varepsilon}} [G_{f\sigma}(\omega + \varepsilon) A_b(\varepsilon) - A_{f\sigma}(\varepsilon) G_b^*(\varepsilon - \omega)]. \tag{10}$$

Note that in Eqs. (8) and (9) $A_{c\sigma}(\varepsilon)$ is the interacting DOS, renormalized by the dilute concentration of Anderson impurities and the $4f$ spins according to Eq. (4). For details of the NCA and its evaluation, see [16]. Equations (4)–(10) form a closed set of self-consistent integral equations. They are solved iteratively, fixing the total electron number per lattice site in the system,

$$n = \sum_\sigma \int d\omega f(\omega) [A_{c\sigma}(\omega) + n_I A_{d\sigma}(\omega)] = n_I, \tag{11}$$

by the chemical potential μ in each step.

Electrical conductivity.—The current operator $\hat{\mathbf{j}}$ can be derived from the continuity equation, $\partial \hat{\rho}_i / \partial t + \nabla \cdot \hat{\mathbf{j}} = 0$, and the Heisenberg equation of motion for the total local charge operator $\hat{\rho}_i$ at site i. Because the impurity Hamiltonians $H_{\rm cf}, H_{\rm df}$ conserve $\hat{\rho}_i$, only c electrons contribute to the current, and one obtains [18] $\hat{\mathbf{j}} = (e/\hbar) \sum_{\mathbf{k}\sigma} \partial \varepsilon_{\mathbf{k}} / \partial \mathbf{k} c^\dagger_{\mathbf{k}\sigma} c_{\mathbf{k}\sigma}$. The linear response conductivity then reads for a local self-energy [18]

$$\sigma = \frac{\pi e^2}{3\hbar V} \sum_{\mathbf{k}\sigma} \int d\omega \left(-\frac{\partial f}{\partial \omega} \right) A^2_{c\sigma}(\mathbf{k}, \omega) \left(\frac{\partial \varepsilon_{\mathbf{k}}}{\partial \mathbf{k}} \right)^2. \tag{12}$$

Results and discussion.—The results of the self-consistent theory, Eqs. (4)–(11), and for the conductivity, Eq. (12), are presented in Figs. 1–3. They allow us to draw a complete picture of the FM semiconductor-metal transition in Gd-doped EuO. The spectral densities per lattice site above and below the transition are shown in Fig. 1. In the paramagnetic, insulating phase the hybridization between d and c electrons necessarily implies the appearance of a conduction electron sideband (Fig. 1, inset), situated below μ and at the same energies inside the semiconducting gap as the impurity d band. The d band (not shown) has a similar width and shape as the c sideband. The combined weight of the c sideband and the d band adjusts itself self-consistently such that it just accommodates the total elec-

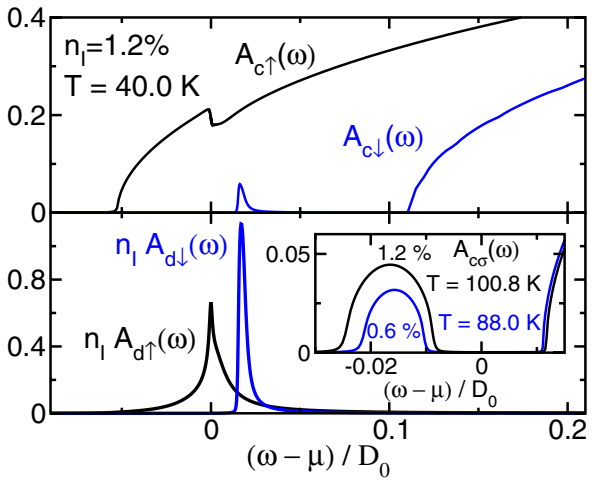

FIG. 1 (color online). Conduction (upper panel) and impurity (lower panel) electron DOS per lattice site for $T \ll T_C$. The impurity concentration is $n_I = 1.2\%$. The metallic phase is fully spin polarized. Inset: c-electron DOS in the paramagnetic phase for $n_I = 1.2\%$, $T = 100.8$ K and for $n_I = 0.6\%$, $T = 88.0$ K. The chemical potential lies in the gap.

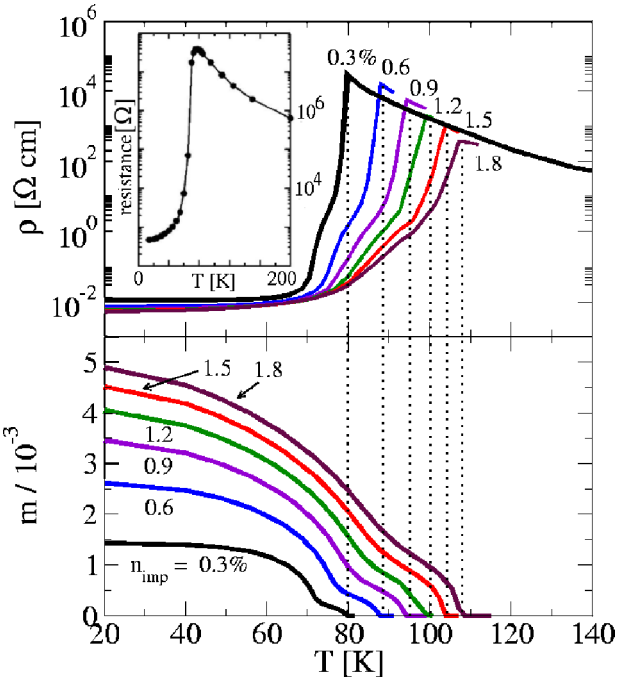

FIG. 2 (color online). Simultaneous FM and semiconductor-metal transition as seen in the T dependence of the magnetization m and of the resistivity $\rho = 1/\sigma$. The Curie temperature depends significantly on the impurity concentration n_I. The inset shows a typical experimental $\rho(T)$ curve, taken from Ref. [4].

tron number, $n = n_I$. Note that the weight of the d band per impurity and spin is $\lesssim 1/2$, because the doubly occupied weight is shifted to $U \to \infty$ [16].

The c-$4f$ exchange coupling $J_{\rm cf}$ induces an effective FM coupling between the electrons of the c-d system. Hence, either the $4f$ or the c-d electron system can drive a FM transition, depending on which of the (coupled) subsystems has the higher T_C. We have chosen $J_{\rm cf}$ (see above) large enough that the transition is driven by the c-d electrons, because this will yield detailed agreement with the experiments [4,7,12]. In this case, T_C is naturally expected to increase with the impurity density n_I. The results for the T-dependent conduction electron magnetization $m(T)$, Eq. (7), and for the doping dependence of T_C are shown in Fig. 2, lower panel, and in Fig. 3, right panel, respectively. It is seen that not only T_C increases with the impurity concentration, in agreement with recent measurements on $Eu_{1-y}Gd_yO_{1-x}$ [7,12], but also that $m(T)$ has a dome-like tail near T_C, before it increases to large values deep inside the FM phase. From our theory this feature is traced back to the mean-field-like 2nd order FM transition of the electron system, while the large dome in the magnetization further below T_C is induced by the FM ordering of the $4f$ system, whose magnetization is controlled by J_{4f} and sets in at lower T. This distinct feature is again in agreement with the experimental findings [7,12] and lends significant support for the present model for $Eu_{1-y}Gd_yO_{1-x}$. We note that the Eu-rich EuO_{1-x} samples of Ref. [12] also show a magnetization tail and a T_C enhancement, suggesting (small) magnetic moments on the O defects. However, the nature of the O defects requires further experimental and theoretical studies. The conduction electron polarization $P(T) = m(T)/n_c(T)$, $n_c(T)$ the conduction electron number per site, does not show this double-dome structure and below T_C increases steeply to $P = 1$ (not shown in Fig. 2). The FM phase is connected with a spin splitting of the c as well as the d densities of states, as shown in Fig. 1. The narrow d band induces a Fano dip structure in the c majority band and a small sideband in the c minority band. Note that for the present scenario the existence of preformed local moments on the impurities, induced by strong Coulomb repulsion U, is essential. Without these moments the transition of the electron system would be purely Stoner-like, and, because of the extremely low conduction

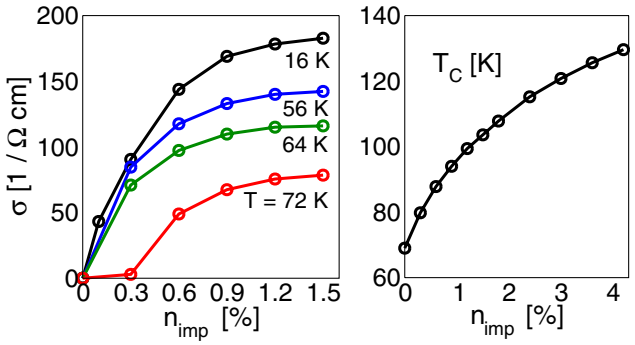

FIG. 3 (color online). Conductivity σ for various temperatures (left panel) and Curie temperature T_C (right panel) as a function of impurity concentration n_I. The data points at $n_I = 0$ in the left panel are extrapolations.

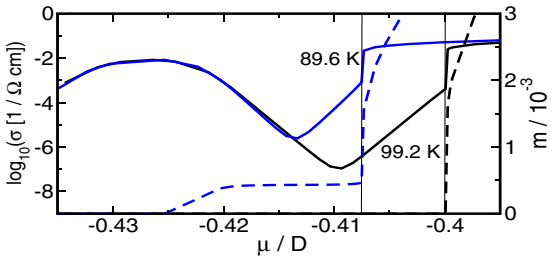

FIG. 4 (color online). Conductivity (solid line) and magnetization (dashed line) as a function of μ for $T = 89.6$ K and $T = 99.2$ K. At the ungated points, $\mu \approx -0.414 D_0$ for $T = 89.6$ K and $\mu \approx -0.410 D_0$ for $T = 99.2$ K, the total electron number per lattice site is equal to the impurity concentration, $n = n_I$.

electron DOS at the Fermi level, its T_C would be far below the Curie temperature of the $4f$ system, so that no doping dependence would be expected [10].

We now discuss the conductivity and the simultaneity of the FM and the SM transitions. In the paramagnetic phase, the system is weakly semiconducting, because μ lies in the gap (Fig. 1, inset). When the FM transition occurs, the impurity d band must acquire a spin splitting in such a way that at least part of the minority d-spectral weight lies above the chemical potential μ, in order to provide a finite magnetization. Since near the transition the spin splitting is small, the majority d band must, therefore, also be shifted to have overlap with μ (Fig. 1), and so must the hybridization-induced c-electron sideband (which eventually merges with the main conduction band for T sufficiently below T_C). This immediately implies a transition to a metallic state, simultaneous with the FM transition, as seen in Fig. 2. Because of the small, but finite thermal occupation of the states around μ, we find that this shifting of spectral weight occurs continuously, which implies the FM semiconductor-metal transition to be of 2nd order (see Fig. 2). The doping n_I dependence of the conductivity is shown in Fig, 3, left panel. It is seen that the metallic transition can be driven by increasing n_I, if $T > T_C(n_I = 0)$.

As an alternative to Gd doping the charge carrier concentration n can be controlled independently of the impurity concentration n_I by varying the chemical potential μ, e.g., by applying a gate voltage to an EuO thin film. The conductivity σ and magnetization m as a function of μ are shown in Fig. 4 for two temperatures. To both sides of the ungated system ($n = n_I$) σ increases exponentially upon changing μ, characteristic for semiconducting behavior. By increasing μ, the FM-metallic transition is finally reached; that is, the magnetization can be switched, in principle, by a gate voltage. The nonmonotonic behavior of σ toward more negative μ reflects the energy dependence of the c sideband. A more detailed study will be presented elsewhere.

To conclude, our theory indicates that in Gd-doped EuO the existence of preformed local moments on the impurity levels inside the semicondicting gap is essential for understanding the distinct shape of the magnetization $m(T)$ near the ferromagnetic semiconductor-metal transition. The FM ordering is driven by these impurity moments which are superexchange coupled via the $4f$ moments of the underlying Eu lattice. This scenario immediately implies an increase of the Curie temperature with the impurity concentration, in agreement with experiments. The double-dome shape of $m(T)$ arises because of the successive ordering of the dilute impurity and of the dense Eu $4f$ systems, as T is lowered. The dynamical accumulation of conduction spectral weight at the chemical potential, induced by the hybridization V and the constraint of an emerging magnetization at the FM transition, implies the FM and the SM transition to be simultaneous and of 2nd order. The magnetization can be switched by applying a gate voltage. This might be relevant for spintronics applications.

We wish to thank T. Haupricht, H. Ott, and H. Tjeng for useful discussions. J. K. is grateful to the Aspen Center for Physics where this work was completed. This work is supported by DFG through No. SFB 608.

[1] M. Oliver *et al.*, Phys. Rev. Lett. **24**, 1064 (1970).
[2] M. Oliver *et al.*, Phys. Rev. B **5**, 1078 (1972).
[3] T. Penney, M. W. Shafer, and J. B. Torrance, Phys. Rev. B **5**, 3669 (1972).
[4] P. B. Steeneken *et al.*, Phys. Rev. Lett. **88**, 047201 (2002).
[5] Y. Shapira, T. Foner, and S. B. Reed, Phys. Rev. B **8**, 2299 (1973).
[6] For a review, see, e.g., M. Imada, A. Fujimori, and Y. Tokura, Rev. Mod. Phys. **70**, 1039 (1998).
[7] H. Ott *et al.*, Phys. Rev. B **73**, 094407 (2006).
[8] A. Schmehl *et al.*, Nat. Mater. **6**, 882 (2007).
[9] R. Schiller, W. Müller, and W. Nolting, Phys. Rev. B **64**, 134409 (2001).
[10] P. Sinjukow and W. Nolting, Phys. Rev. B **68**, 125107 (2003); Phys. Rev. B **69**, 214432 (2004).
[11] V.-C. Lee and L. Liu, Phys. Rev. B **30**, 2026 (1984).
[12] T. Matsumoto *et al.*, J. Phys. Condens. Matter **16**, 6017 (2004).
[13] D. I. Golosov, Phys. Rev. B **71**, 014428 (2005).
[14] M. D. Kapetanakis, A. Manousaki, and I. E. Perakis, Phys. Rev. B **73**, 174424 (2006); M. D. Kapetanakis and I. E. Perakis, Phys. Rev. B **75**, 140401(R) (2007).
[15] N. Grewe and H. Keiter, Phys. Rev. B **24**, 4420 (1981); Y. Kuramoto, Z. Phys. B **53**, 37 (1983).
[16] T. A. Costi, J. Kroha, and P. Wölfle, Phys. Rev. B **53**, 1850 (1996).
[17] S. Kirchner and J. Kroha, J. Low Temp. Phys. **126**, 1233 (2002).
[18] H. Schweitzer and G. Czycholl, Phys. Rev. Lett. **67**, 3724 (1991); T. Pruschke, M. Jarrell, and J. Freericks, Adv. Phys. **44**, 187 (1995).